A Least-Square-based RMRAC for Grid-tied Voltage Source Inverters with LCL Filter

Paulo J. D. de O. Evald
Intelligent Systems and Control Group
Federal University of Pelotas
Pelotas, Brazil
email: paulo.evald@gmail.com

Guilherme V. Hollweg, Lucas C. Borin, Everson Mattos,
Rodrigo V. Tambara, and Vinicius F. Montagner
Group of Power Electronics and Control
Federal University of Santa Maria

***Abstract*—Renewable energy generation systems commonly use LCL filters as interfaces between them and the grid, aiming to reduce the harmonic content of Voltage Source Inverters. However, the LCL filter presents a relevant resonance peak that can lead the closed-loop to instability. Therefore, aiming to mitigate it, and provide an adequate current injection into the grid, in this paper is presented a Least-Squares-based Robust Model Reference Adaptive Controller. The proposed control strategy can track reference currents fast, while rejecting exogenous disturbances without needing additional control loops. Besides, the controller is robust enough to consider the LCL filter as a first order transfer function during its design, which allows it to use a first order reference model, reducing the complexity inherent to adaptive control strategies. Simulation results are presented to discuss the feasibility of a proposed control strategy for grid-injected current control.**

***Index Terms*—Adaptive Controllers, Automatic Controllers, Grid-tied Power Systems, Auto-tuning Controllers.**

I. Introduction

Grid-tied voltage source inverters (VSI) with LCL filters are one of the most common topologies used in renewable energy systems [1]. This filtering strategy allows attenuating harmonics from the pulse-width modulation voltages generated by the inverter, at the price of a more careful damping of the resonance of the LCL filter. This damping can be carried out passively, including resistance in the filter, or actively, by means of feedback control techniques. The last option is more interesting to keep the high efficiency of the converter, but demands a more careful control design.

In the context of grid current control strategies applied to grid-tied voltage source inverters with LCL filter, one has the virtual resistance approach, where the LCL capacitor filter can be used in feedback, in order to emulate a physical resistance that attenuates the filter resonance [1]. This technique can be used associated with Proportional-Resonant controllers, aiming to ensure good tracking of sinusoidal grid current references and attenuation of grid voltage harmonics [2]. More recently, state feedback techniques extensible for arbitrary number of Resonant Controllers have been developed, where the state feedback grid current control gains have been designed by means of linear matrix inequalities [3], [4]. Other relevant control strategies for this application are: Sliding Mode Controller [5], High Order Sliding Mode Controller [6], Predictive Controller [7], [8], Cascade controller [9], Resonant Controller [10], among others.

However, a common point between the above-mentioned works is the use of fixed (i.e. time-invariant) control gains during the real time operation of the controller. Although this makes the control implementation simpler than time-varying control gains, it can lead to conservative performances, mainly under larger parameter uncertainties or disturbances, and a better trade-off between performance and stability can be achieved by using adaptive controllers. In the literature, there are some interesting adaptive control systems for grid-injection current control, such as: Robust Model Reference Adaptive Control (RMRAC) [11], Adaptive Sliding Mode Control [12], [13], [14], Robust Adaptive Super-Twist Sliding Mode Control [15], Robust Model Reference-based Adaptive PI controller [16], Robust Adaptive PI controller [17], Robust Adaptive One Sample Ahead Preview controller [18], among others. However, these controllers use a modified Gradient algorithm to adjust its gains online, which is a low computational burden technique. On the other hand, Least Squares (LS)-based algorithms can provide a faster adaptation than Gradient algorithms, at the price of an increase in controller complexity. Nevertheless, the computational burden addition is justifiable by controller improvements, which can have its structure reduced using the strategy of modelling simplification, introduced in [11]. Therefore, this paper presents an LS-based RMRAC for grid-injection current control of a VSI with LCL filter.

The rest of this work is organised as follows: Section II shows the LCL filter model, and Section III presents the LS-based RMRAC for grid-side current control loop. Next, Section IV provides the simulation results, and the conclusions of this work are given in Section V.

II. LCL filter model

A renewable energy generation system is composed, basically, of a primary power source (the clean energy source, such as sun or wind), a VSI, an LCL filter, the grid, and a control system. The energy conversion process in detail is outside the scope of this work. Here, the energy source is generalised, described by V_{cc}, which is transformed to AC currents in the VSI, using a proper controller. However, VSI dynamics impose

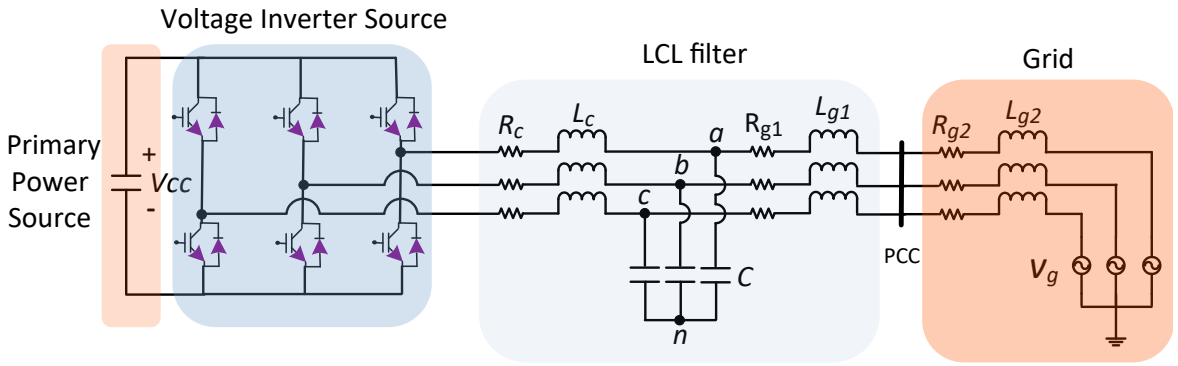

Fig. 1. Grid-tied VSI with LCL filter.

a harmonic content onto the currents. Thereby, current flows through an LCL filter before it is injected into the grid. From the outside, it is used as the interface between the primary power source and the electrical grid. This output filter is composed of two inductors (one at converter-side, L_c, and one at grid-side, L_{g1}) and one capacitor, C, as shown in Fig. 1. The filter inductors have a parasitic resistance associated, which is represented by R_c and R_{g1} for L_c and L_{g1}, respectively. The grid is considered predominantly inductive, described as the three-phase sinusoidal source as V_g, whose impedance is given by $R_{g2} + L_{g2}$. Furthermore, the equivalent LCL filter circuit is given by Thevenin equivalent in relation to the PCC (Point on Common Coupling) [19], where the grid voltages are measured.

Although the use of the LCL filter reduces harmonic content, its three-phase model is strongly coupled [17], which makes the current control design a nontrivial task. Thereby, the Clarke Transformation [20] is employed to decouple the three-phase system into three independent models, in $\alpha\beta 0$ coordinates. Considering the equilibrated phases, 0 coordinate can be disregarded, because there is no way for current flow, simplifying it to two decoupled identical single-phase models [21], as shown, for α coordinate, where i_c, v_c and i_g are converter-side currents, capacitor voltage and grid-side currents, respectively. Besides, $u(s)$ is the voltage synthesised by the converter. The transfer function of the LCL filter, $G(s)$, is obtained considering the VSI disconnected from the grid, because it is treated as an exogenous disturbance in the control design.

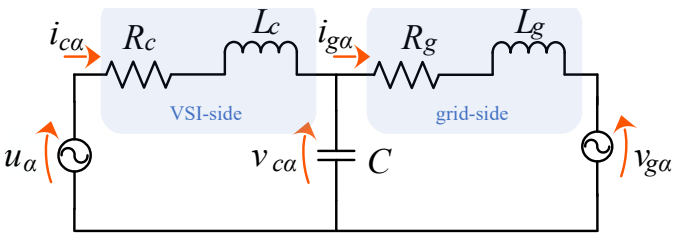

Fig. 2. Equivalent circuit of grid-tied VSI with LCL filter.

Applying Kirchhoff's circuit laws to the single-phase circuit, the LCL filter transfer function, for α and β coordinates, is

$$G(s) = \frac{i_g(s)}{u(s)} = \frac{1}{a_1 s^3 + a_2 s^2 + a_3 s + a_4}, \tag{1}$$

where $a_1 = L_g L_c C$, $a_2 = (R_g L_c + R_c L_g)C$, $a_3 = L_c + L_g + R_g R_c C$ and $a_4 = R_g + R_c$.

A. Simplification of LCL filter

Note that (1) has a relative degree equal to 3. When discretised with Zero Order Hold (ZOH), its relative degree is 2 [15]. Aiming to simplify the adaptive control system, the LCL filter is modelled as a first order transfer function, only for controller design, neglecting the capacitor dynamics, as originally shown in [11]. Note that this model simplification can only be used if the controller is robust enough to deal with neglected dynamics, while faced with exogenous disturbances, grid uncertainties, and plant parameter variations. The resulting transfer function, considered as a nominal transfer function $G_0(s)$ for controller design, is

$$G_0(s) = \frac{1}{(L_c + L_g)s + R_c + R_g}. \tag{2}$$

III. LS-BASED RMRAC

Consider a single-input single-output plant, $G(z)$, given by

$$G(z) = G_0(z)\left[1 + \mu_1 \Delta_m(z)\right] + \mu_2 \Delta_a(z), \tag{3}$$

where $\mu_1\Delta_m$ and $\mu_2\Delta_a$ are related to the multiplicative and additive unmodelled dynamics, respectively, being μ_1 and μ_2 both scalars. Thereby, the plant output, y, is given by

$$y = G_0(z)u + \mu\eta, \tag{4}$$

where u is the plant input, $\eta = \Delta G(z)u$ and $\Delta G(z) = G_0(z)\Delta_m(z) + \Delta_a(z)$, being $\Delta G(z)$ the plant uncertainties. The nominal part of the plant is given by

$$G_0(z) = k_p \frac{N(z)}{D(z)}, \tag{5}$$

which have to respect the following assumptions:
I: k_p is the plant gain, whose sign is known, but its value can be unknown;
II: $N(z)$ is a monic polynomial, which can be unknown,

whose order is m;
III: $D(z)$ is a monic polynomial, which can be unknown, whose order is n, where $n > m$;
IV : the coefficients of $N(z)$ and $D(z)$ are unknown.

In direct adaptive control strategies, the aim of the controllers is to track, as close as possible, the reference model output $y_m(k)$. Thus, a reference model, $W_m(k)$, is chosen by the designer. It is described by

$$W_m(z) = k_m \frac{1}{D_m(z)}, \tag{6}$$

where k_m is a gain, and $D_m(z)$ is a monic polynomial, with order $n - m$. The $W_m(k)$ input is the reference signal, r.

The control action, $u(k)$, is extracted from $\boldsymbol{\theta}^T(k)\boldsymbol{\omega}(k)+r = 0$, where $\boldsymbol{\omega}(k)$ is an auxiliary vector, which is given by

$$\boldsymbol{\omega}^T(k) = [\ u(k)\ y(k)\ V_s(k)\ V_c(k)\ ], \tag{7}$$

being $V_s(k)$ and $V_c(k)$, the phase and quadrature of the fundamental harmonics of the grid, which are estimated to feedback the disturbance rejection terms. Besides, $\boldsymbol{\theta}(k)$ is the adaptive gains vector, formed by

$$\boldsymbol{\omega}^T(k) = [\ \theta_u(k)\ \theta_y(k)\ \theta_s(k)\ \theta_c(k)\ ], \tag{8}$$

where $\theta_u(k)$, $\theta_y(k)$, $\theta_s(k)$, and $\theta_c(k)$ are related to $u(k)$, $y(k)$, $V_s(k)$, and $V_c(k)$, respectively.

For gain adaptation, the Least Square algorithm was utilised [22],

$$\boldsymbol{\theta}(k+1) = \boldsymbol{\theta}(k) - T_s\sigma(k)\boldsymbol{P}(k)\boldsymbol{\theta}(k) - T_s\boldsymbol{P}(k)\frac{\boldsymbol{\zeta}(k)\epsilon(k)}{m^2(k)}, \tag{9}$$

where $\boldsymbol{P}(k)$ is the covariance matrix, and ϵ is the augmented error, described as

$$\epsilon(k) = e_1(k) + \boldsymbol{\theta}^T(k)\boldsymbol{\zeta}(k) - \nu(k), \tag{10}$$

where ν is the control signal filtered by reference model,

$$\nu = W_m(z)u, \tag{11}$$

and $\zeta(k)$ is the auxiliary vector filtered by reference model [22],

$$\zeta = W_m(z)\omega. \tag{12}$$

In addition, the tracking error $e_1(k)$ is given by the difference between model reference and plant outputs,

$$e_1(k) = y_m(k) - y(k). \tag{13}$$

The covariance matrix $\boldsymbol{P}(k)$ concerns about convergence rate of the gains. In this work, the following algorithm is adopted,

$$\boldsymbol{P}(k+1) = \boldsymbol{P}(k) - T_s\boldsymbol{P}(k)\boldsymbol{\zeta}(k)\boldsymbol{\zeta}^T(k)\boldsymbol{P}(k) + T_s\beta\boldsymbol{\iota}, \tag{14}$$

where $\boldsymbol{\iota}$ is a matrix of ones, and β is a constant. It is highlighted that the term $T_s\beta\boldsymbol{\iota}$ is used to avoid $\boldsymbol{P}$ stagnating in zero.

The controller is robustified with the σ-modification, to avoid parameter drifting. It is given by

$$\sigma(k) = \begin{cases} 0 & \text{if} \quad \|\boldsymbol{\theta}(k)\| < M_0 \\ \sigma_0(\frac{\|\boldsymbol{\theta}(k)\|}{M_0} - 1) & \text{if} \quad M_0 \leq \|\boldsymbol{\theta}(k)\| < 2M_0, \\ \sigma_0 & \text{if} \quad \|\boldsymbol{\theta}(k)\| \geq 2M_0 \end{cases} \tag{15}$$

where σ_0 is the maximum value of the modification function, and $M_0 > \|\boldsymbol{\theta}^*\|$ is the upper limit of $\boldsymbol{\theta}(k)$ norm, which can be securely oversized due to lack of knowledge of $\|\boldsymbol{\theta}^*\|$ [18].

Besides, a majorant signal $m^2(k)$ is also incorporated into the algorithm, aiming to improve its robustness. The dynamics of this signal are updated as

$$m^2(k) = 1 + \boldsymbol{\zeta}^T(k)\boldsymbol{\zeta}(k). \tag{16}$$

IV. Simulation Results

The simulation was carried out in the PSIM simulator. The grid frequency, line voltage range and DC bus voltage were set to 60 Hz, 110 V and 500 V, respectively. Besides, the VSI switching frequency and the controller's sampling frequency were both set to 5040 Hz. Moreover, the grid and LCL filter parameters are shown in Table I.

TABLE I
Grid and LCL filter parameters.

Symbol	Parameter	Value
L_c	Converter-side inductance	1 mH
R_c	Converter-side parasitic resistance	50 mΩ
C	Capacitance of LCL filter	62 μF
L_{g1}	Grid-side inductance of LCL filter	0.3 mH
R_g	Grid-side parasitic resistance	50 mΩ
L_{g2}	Grid inductance	0.50 mH

The controller parameters were chosen empirically, based on designer experience, where the aim was obtaining fast current tracking, while avoiding excessive overshoots (up to 35 A). However, if the gains are chosen far from a solution set, a high overshoot is observed in the initial transient regime. To avoid it, a previous simulation was performed, using random gain initialisation, and reference currents of 25 A in sine form with a frequency of 60 Hz. Therefore, the final gains of this simulation were used to initialise the gains of the presented simulation. Although simple, this method provides a satisfactory solution set, avoiding excessive overshoot in the initial transient. The resulting gains are

$$\boldsymbol{\theta}_\alpha(0) = \begin{bmatrix} -1.07 \\ -1.33 \\ 1.14 \\ 1.58 \end{bmatrix} \quad , \quad \boldsymbol{\theta}_\beta(0) = \begin{bmatrix} -9.33 \\ -1.39 \\ 7.92 \\ 6.65 \end{bmatrix}.$$

The designed parameters of the controller are: $\boldsymbol{P}(0) = 500\boldsymbol{I}$, $\boldsymbol{\beta} = 50$, $\sigma_0 = 0.1$, $M_0 = 15$, and $m^2(0) = 4$. The reference model was chosen to have unit gain in stationary regime, and it is identical for both controllers (in α and β), given by

$$W_m(z) = \frac{0.7}{z - 0.3}. \tag{17}$$

Simulation consists of the following events:

1) During 0.05 s the controller does not actuate, because the Kalman filter [23] is synchronising with the grid;
2) From 0.05 s to 0.1 s, the reference alternate currents have an amplitude of 25 A, and the controller starts to act, being synthesised by converter using Space Vector Modulation [24];
3) From 0.1 s, the reference alternate current amplitude is increased to 35 A;
4) At 0.2 s, a parametric variation into grid-side impedance is imposed, changing it from 0.3 mH to 1.3 mH, turning the grid weaker;
5) The VSI is disconnected at 0.35 s.

Figure 3 shows the three-phase grid-injected currents, in abc coordinates. Note that using the gain initialisation strategy, excessive overshoot was avoided in the initial transient. Besides, the controller maintained the currents at the desired amplitude during all tests, for different loads, and grid conditions. To better analyse the events of this simulation, Fig. 4, 5, and 6 present the load change, parametric variation instant, and steady state regime, respectively.

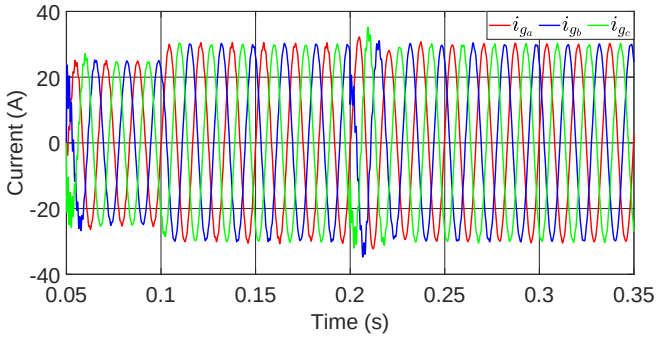

Fig. 3. Grid-injected currents.

Note that in the load change, from 25 A to 35 A, shown in Fig 4, the controller presented fast current tracking. In less than one complete grid cycle, the currents achieve, smoothly, the new condition. As can be seen, no overshoot occurred, and only a small distortion was observed in this transient.

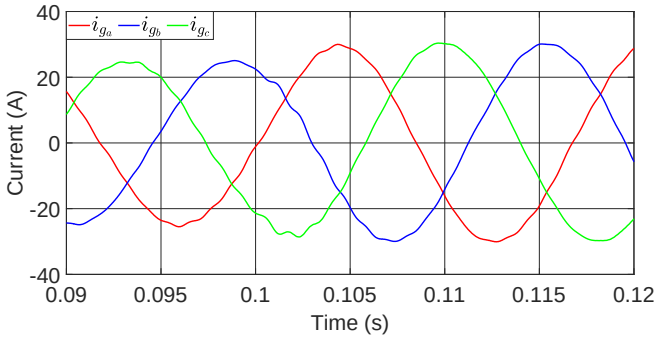

Fig. 4. Grid-injected currents (load change).

Moreover, during the parametric variation transient, shown in Fig. 5, the grid condition variation was compensated by less than 30 ms. Again, no relevant overshoot is observed, but during this transient, the currents were distorted, while the gains are readapted by a least-squares algorithm.

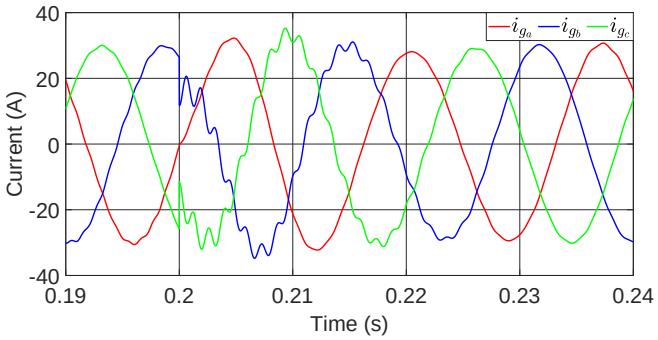

Fig. 5. Grid-injected currents (parametric variation).

In steady state, shown in Fig. 6, the currents are properly injected into the grid, with low Total Harmonic Content (THD), around 1.60%, 1.73%, and 1.53% for i_{ga}, i_{gb}, and i_{gc}, respectively, which is far from limit imposed by IEEE 1548 standard (5%).

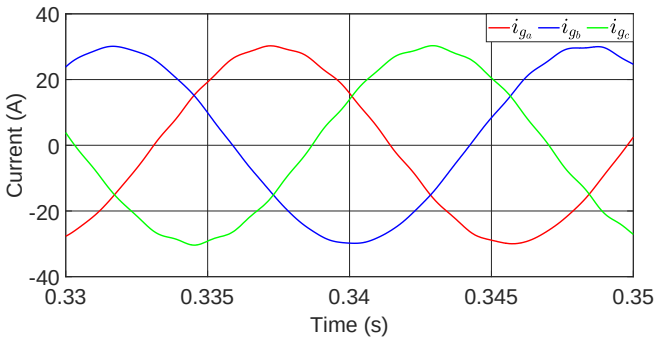

Fig. 6. Grid-injected currents (steady state).

Thus, the controller presented satisfactory performance for grid-side current control of the VSI with LCL filter. For a deeper discussion of its performance, the $\alpha\beta$ results are also discussed. Figure 7 shows the current tracking, where the plant output, y, has to track the reference model output, y_m, as close as possible. Naturally, these results are similar to abc currents, because the difference between them is only the representation, provided by the Clarke transformation, which preserves amplitude and frequency.

The tracking errors are presented in Fig 8, where it can be seen that the greater tracking errors were due to the initial transient, load change and parametric variation. In steady state, the tracking error in both coordinates converged to a residual set, which did not go to zero due to unmodelled dynamics, such as VSI switching and time delay of digital implementation. The average errors were 0.0798 A and -0.0107 A, which indicates the current tracking in the overall

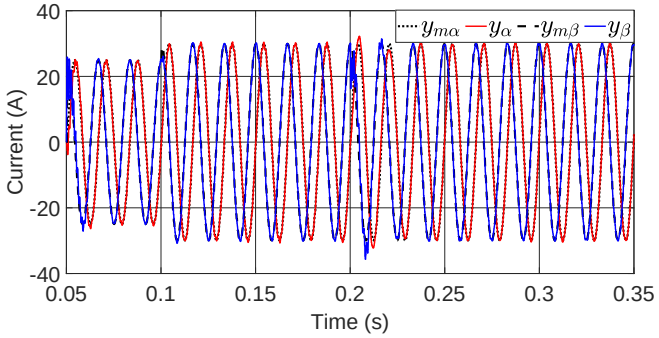

Fig. 7. Grid-injected currents in $\alpha\beta$ coordinates.

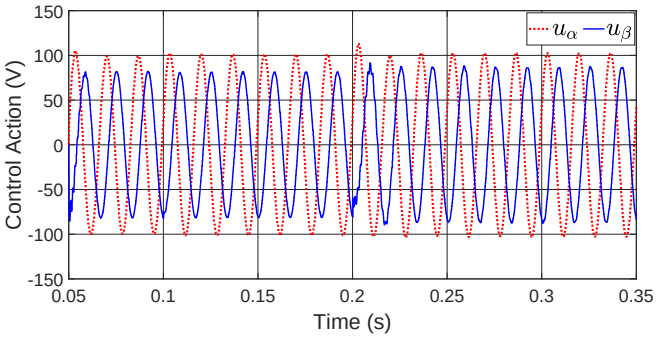

Fig. 9. Control actions in $\alpha\beta$ coordinates.

test was very close to the reference, being expressive only during the transient regimes. Besides, Root Mean Squared (RMS) errors were 1.0152 A and 1.3692 A for α and β coordinates, respectively, corroborating the previous analysis.

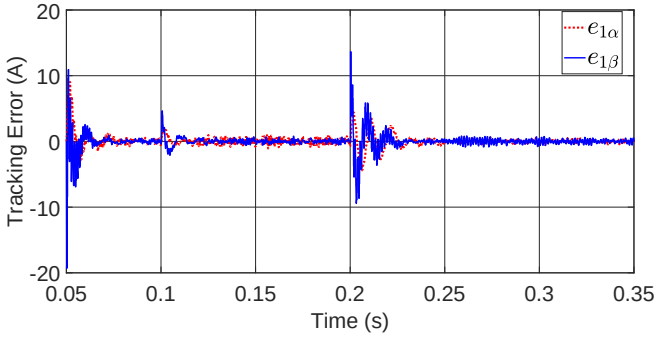

Fig. 8. Tracking errors in $\alpha\beta$ coordinates.

The control actions are shown in Fig. 9. Note that the Least-Squares-based RMRAC did not require relevant voltage to reject exogenous disturbance, while maintaining the current tracking. DC voltage bus was 500 V, while the control action, in α and β coordinates, did not exceed 110 V. The higher values were associated with grid condition changes, but it did not impose relevant additional effort. As can be seen, in this transient, the control actions were around 120 V, far from the available voltage.

The adaptive gains in α and β coordinates are shown in Fig. 10 and 11, respectively. As expected, the gains were adapted more intensively for each system perturbation, tending to be accommodated in steady state.

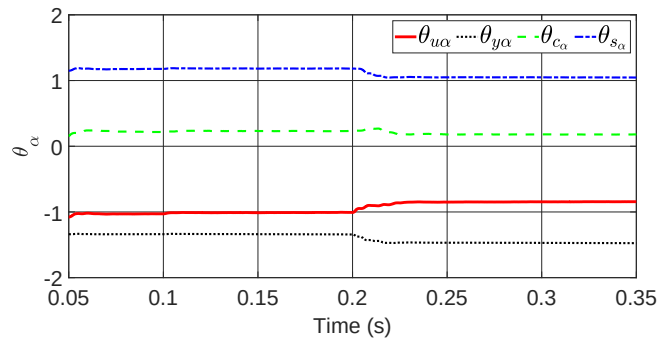

Fig. 10. Adaptive gains in α coordinate.

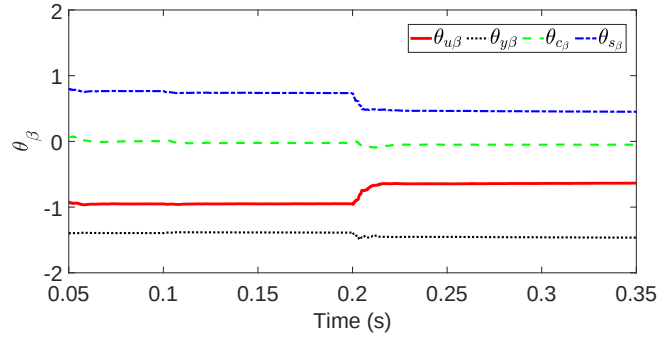

Fig. 11. Adaptive gains in β coordinates.

V. Conclusion

In this paper was presented a Least-Squared-based Robust Model Reference Adaptive Controller for grid-injected current control of a VSI with LCL filter. The proposed control strategy is robust enough to be designed considering the LCL filter model as a first order transfer function, which allows using a first order reference model, simplifying the adaptive control system. Besides, due to the nature of the LS algorithm, the grid-side currents were fast regulated after each system perturbation, achieving a steady state in less than 30 ms and 23 ms for load change and grid impedance change, respectively. Furthermore, the average tracking errors were 0.0798 A and -0.0107 A, for α and β coordinates, respectively, while the RMS tracking errors were 1.0152 A and 1.3692 A for α and β coordinates. Furthermore, the harmonic content in the three-phase currents respected the IEEE 1548 standard, with a THD of 1.60%, 1.73%, and 1.53% for i_{ga}, i_{gb}, and i_{gc}, respectively. In the future work, a methodology for parametrisation will be provided, and tests in a laboratory-scale prototype will be performed, aiming to validate the simulation results experi-

mentally.

REFERENCES

[1] R. Teodorescu, M. Liserre, and P. Rodríguez, *Grid Converters for Photovoltaic and Wind Power Systems*, ser. Wiley - IEEE. John Wiley & Sons, 2011.

[2] J. Dannehl, M. Liserre, and F. Fuchs, "Filter-based active damping of voltage source converters with LCL filter," *IEEE Transactions on Industrial Electronics*, vol. 58, no. 8, pp. 3623–3633, August 2011.

[3] L. A. Maccari, Jr., J. R. Massing, L. Schuch, C. Rech, H. Pinheiro, R. C. L. F. Oliveira, and V. F. Montagner, "LMI-based control for grid-connected converters with LCL filters under uncertain parameters," *IEEE Transactions on Power Electronics*, vol. 29, no. 7, pp. 3776–3785, July 2014.

[4] G. G. Koch, C. R. D. Osório, H. Pinheiro, R. C. L. F. Oliveira, and V. F. Montagner, "Design procedure combining linear matrix inequalities and genetic algorithm for robust control of grid-connected converters," *IEEE Trans. on Industry Applications*, vol. 56, no. 2, pp. 1896–1906, 2019.

[5] Q. Teng, G. Xu, X. Zheng, H. Mai, X. Ma, and Y. Wang, "A novel sliding mode observer-based compound sliding mode current control with active damping for single phase grid-tied inverter system in weak grid," *International Journal of Electrical Power & Energy Systems*, vol. 141, p. 108117, 2022.

[6] M. Barzegar-Kalashani, B. Tousi, M. A. Mahmud, and M. Farhadi-Kangarlu, "Higher-order sliding mode current controller for grid-connected distributed energy resources with lcl filters under unknown grid voltage conditions," *IET Generation, Transmission & Distribution*, vol. 16, no. 8, pp. 1592–1606, 2022.

[7] M. Rossi, P. Karamanakos, and F. Castelli-Dezza, "An indirect model predictive control method for grid-connected three-level neutral point clamped converters with *lcl* filters," *IEEE Transactions on Industry Applications*, vol. 58, no. 3, pp. 3750–3768, 2022.

[8] R. Heydari, H. Young, F. Flores-Bahamonde, S. Vaez-Zadeh, C. Gonzalez-Castano, S. Sabzevari, and J. Rodriguez, "Model-free predictive control of grid-forming inverters with *lcl* filters," *IEEE Transactions on Power Electronics*, vol. 37, no. 8, pp. 9200–9211, 2022.

[9] K. Kumari and A. K. Jain, "Cascaded control for lcl filter based grid-tied system with reduced sensors," *IET Power Electronics*, p. 1=14, 2022.

[10] D. Khan, P. Hu, S. Habib, M. Waseem, Z. Lin, and E. M. Ahmed, "A resonant damping control and analysis for lcl-type grid-connected inverter," *Energy Reports*, vol. 8, pp. 911–928, 2022.

[11] P. J. D. O. Evald, R. V. Tambara, and H. A. Gründling, "A direct discrete-time reduced order robust model reference adaptive control for grid-tied power converters with lcl filter," *Brazilian Journal of Power Electronics*, vol. 25, no. 3, pp. 361–372, 2020.

[12] G. V. Hollweg, P. J. D. O. Evald, E. Mattos, R. V. Tambara, and H. A. Gründling, "Feasibility assessment of adaptive sliding mode controllers for grid-tied inverters with lcl filter," *Journal of Control, Automation and Electrical Systems*, vol. 33, no. 2, pp. 434–447, 2022.

[13] G. V. Hollweg, P. J. D. de Oliveira Evald, D. M. C. Milbradt, R. V. Tambara, and H. A. Gründling, "Design of continuous-time model reference adaptive and super-twisting sliding mode controller," *Mathematics and Computers in Simulation*, vol. 201, p. 215–238, 2022.

[14] G. Vieira Hollweg, P. Dias de Oliveira Evald, R. Varella Tambara, and H. Abílio Gründling, "Adaptive super-twisting sliding mode for dc-ac converters in very weak grids," *International Journal of Electronics*, no. just-accepted, 2022.

[15] G. V. Hollweg, P. J. D. de Oliveira Evald, R. V. Tambara, and H. A. Gründling, "A robust adaptive super-twisting sliding mode controller applied on grid-tied power converter with an lcl filter," *Control Engineering Practice*, vol. 122, p. 105104, 2022.

[16] P. J. D. O. Evald, G. V. Hollweg, R. V. Tambara, and H. A. Gründling, "Lyapunov stability analysis of a robust model reference adaptive pi controller for systems with matched and unmatched dynamics," *Journal of the Franklin Institute*, vol. 359, no. 13, pp. 6659–6689, 2022.

[17] P. J. D. O. Evald, V. Hollweg, R. V. Tambara, and H. A. Gründling, "A new discrete-time pi-rmrac for grid-side currents control of grid-tied three-phase power converter," *International Transactions on Electrical Energy Systems - Special Issue: Control and Power in Renewable Energy Systems*, vol. 31, no. 10, p. e12982, 2021.

[18] D. M. C. Milbradt, G. V. Hollweg, P. J. D. de Oliveira Evald, W. B. da Silveira, and H. A. Gründling, "A robust adaptive one sample ahead preview controller for grid-injected currents of a grid-tied power converter with an lcl filter," *International Journal of Electrical Power & Energy Systems*, vol. 142, p. 108286, 2022.

[19] P. J. D. O. Evald, V. Hollweg, R. V. Tambara, and H. A. Gründling, "A discrete-time adaptive pi controller for grid-connected voltage source converter with lcl filter," *Brazilian Journal of Power Electronics*, vol. 26, no. 1, pp. 19–30, 2021.

[20] W. C. Duesterhoeft, M. W. Schulz, and E. Clarke, "Determination of instantaneous currents and voltages by means of alpha, beta, and zero components," *Transactions of the American Institute of Electrical Engineers*, vol. 70, no. 2, pp. 1248–1255, 1951.

[21] P. J. D. O. Evald, R. V. Tambara, and H. A. Gründling, "A discrete-time robust mrac applied on grid-side current control of a grid-connected three-phase converter with lcl filter," *ELECTRIMACS 2019: Selected Papers-Volume 1*, pp. 45–57, 2020.

[22] P. A. Ioannou and J. Sun, ***Robust adaptive control***. Courier Corporation, 2012.

[23] R. Cardoso, R. F. de Camargo, H. Pinheiro, and H. A. Gründling, "Kalman filter based synchronisation methods," *IET Generation, Transmission & Distribution*, vol. 2, no. 4, pp. 542–555, 2008.

[24] L. Michels, R. De Camargo, F. Botteron, H. Grüdling, and H. Pinheiro, "Generalised design methodology of second-order filters for voltage-source inverters with space-vector modulation," *IEE Proceedings-Electric Power Applications*, vol. 153, no. 2, pp. 219–226, March 2006.